

# Robust Dynamic Mode Decomposition

Amir Hossein Abolmasoumi, Marcos Netto, *Member, IEEE*, and Lamine Mili, *Life Fellow, IEEE*

**Abstract**—The paper develops a robust estimation method that makes the dynamic mode decomposition method resistant to outliers while being fast to compute and statistically efficient (i.e. accurate) at the Gaussian and non-Gaussian thick tailed distributions. The proposed robust dynamic mode decomposition (RDMD) is anchored on the theory of robust statistics. Specifically, it relies on the Schweppe-type Huber generalized maximum-likelihood estimator that minimizes a convex weighted Huber loss function, where the weights are calculated via projection statistics, thereby making the proposed RDMD robust to outliers, whether vertical outliers or bad leverage points. The performance of the proposed RDMD is demonstrated numerically using canonical models of dynamical systems. Simulation results reveal that it outperforms several other methods proposed in the literature, including the one based on the least trimmed squares estimator.

**Index Terms**—Dynamic mode decomposition, outlier detection, robust estimation, robust statistics, robust regression.

## I. INTRODUCTION

THE sustained growth of data acquisition across all areas of human activity is a key driver for the research and development of data science methods [1], [2]. This is especially the case for complex dynamical systems for which data are abundant and first principles models are difficult to obtain. Along these lines, Dynamic Mode Decomposition (DMD) is a numerical method originally proposed by Schmid and Sesterhenn [3] for the data-driven modeling and analysis of dynamical systems. The DMD stands out among the existing numerical methods because of its connection with the Koopman operator theory [4], which reconciles data analysis and the mathematical knowledge of dynamical systems. The reader is referred to [5], [6] for more details. The DMD has become mainstream for the data-driven modeling of dynamical systems, with applications in fluid mechanics [4], electric power grids [7], neuroscience [8], finance [9], climate science [10], and transportation [11], to name a few.

As shown in Section II-B, the original numerical procedure for the DMD [3] makes use of the least-squares estimator,

which is also utilized in all important DMD variants tailored to specific classes of dynamical systems. Examples include but are not limited to the multiresolution DMD [10], the DMD with control [12], the Hankel DMD [13], and the tensor-based DMD [14]. But it is well known that the least-squares estimator is not a robust estimator. Following standard definitions in robust statistics, we define *robustness* as insensitivity to deviations from the assumptions [15]. One assumption that is typically violated in practice is the assumed probability distribution of the observations. In this respect, an *outlier* is defined as a data point that does not satisfy that assumption—that is, it is distant from the majority of the point cloud [16]. In practice, outliers occur because of instrumentation/communications errors or experimental setup, among others. Now, it is well known that the least-squares estimator produces strongly biased results in the presence of a single outlier [17]. Moreover, it quickly loses its statistical efficiency when the tails of the distribution of the observations become slightly thicker than the Gaussian ones.

The numerical procedures' vulnerability to measurement noises, non-Gaussian noise, and outliers is of great concern for practitioners. This fact motivated several independent investigations on the DMD outcome's accuracy in capturing underlying system dynamics directly from the data [18]–[20]. Hence, the bias introduced by the measurement noises was addressed in [21]. In addition, the bias resultant from processing snapshots asymmetrically was addressed in [22]. However, the numerical procedures' vulnerability to outliers is a more challenging problem to tackle. An optimized numerical procedure that is less numerically sensitive to deviations from the assumptions was originally developed in [23] and followed by others [24]. From the standpoint of the theory of robust statistics, though they provide superior numerical performance compared to the original DMD [3], optimized numerical procedures [23], [24] are not robust to outliers. A numerical procedure robust to outliers was proposed in [25], based on the Least Trimmed Squares (LTS) estimator. Specifically, authors have considered the trimmed M-estimators introduced by Rousseeuw [26] while using the Huber  $\rho$ -function because of its convexity; however, they have not used the method of projection statistic as proposed in this paper. Also, such a high-breakdown estimator is difficult to implement and slow to calculate.

In this paper, we develop a fast numerical procedure to make the DMD robust to outliers, even in position of leverage. Leverage points are measurements whose projection on the factor space are outliers [16], [27]. The proposed method, referred to as Robust DMD (RDMD), is based on the Schweppe-type Huber Generalized Maximum-likelihood (SHGM) estimator that can bound the influence of outliers while maintaining good statistical efficiency at the Gaussian and thick-

This work was authored in part by the National Renewable Energy Laboratory (NREL), operated by Alliance for Sustainable Energy, LLC, for the U.S. Department of Energy (DOE) under contract no. DE-AC36-08GO28308. This work was supported by the Laboratory Directed Research and Development (LDRD) program at NREL. The views expressed in the article do not necessarily represent the views of the DOE or the U.S. Government. The U.S. Government and the publisher, by accepting the article for publication, acknowledges that the U.S. Government retains a nonexclusive, paid-up, irrevocable, worldwide license to publish or reproduce the published form of this work, or allow others to do so, for U.S. Government purposes.

Amir H. Abolmasoumi is with the Electrical Engineering Department, Arak University, Arak, 38156879, Iran, and was a visiting scholar with the Bradley Department of Electrical and Computer Engineering, Virginia Polytechnic Institute and State University, Falls Church, VA 22043, USA. M. Netto is with the Power Systems Engineering Center, NREL, Golden, CO 80401, USA. L. Mili is with the Bradley Department of Electrical and Computer Engineering, Virginia Polytechnic Institute and State University, Falls Church, VA 22043, USA. Corresponding author: a-abolmasoumi@araku.ac.ir.

tailed distributions [27]–[32]. The proposed SHGM estimator minimizes a convex Huber loss function that incorporates weights, which are calculated using projection statistics. The performance of the RDMD is examined on a collection of canonical models of dynamical systems, including the Van der Pol oscillator and a family of slow-manifold nonlinear systems. The proposed RDMD is compared via simulations to several other methods [22], [24], [25]. It is demonstrated that it has good robustness and high statistical efficiency under Gaussian and non-Gaussian noise.

The paper is organized as follows. Section II briefly establishes the connection between the Koopman operator and DMD; two numerical procedures for DMD [33], [34] are outlined. Section III develops the proposed RDMD method, which is the main contribution of this paper. Section IV discusses the numerical results, and Section V concludes the paper.

## II. PRELIMINARIES

### A. Koopman Operator

Let us consider an autonomous dynamical system evolving on a finite,  $n$ -dimensional manifold  $\mathbb{X}$  given by

$$\mathbf{x}[k] = \mathbf{F}(\mathbf{x}[k-1]), \text{ for discrete-time } k \in \mathbb{Z}, \quad (1)$$

where  $\mathbf{x} \in \mathbb{X}$  is the state, and  $\mathbf{F} : \mathbb{X} \rightarrow \mathbb{X}$  is a nonlinear vector-valued map. In what follows, we introduce the Koopman operator for discrete-time dynamical systems.

Let  $g(\mathbf{x})$  be a scalar-valued function defined in  $\mathbb{X}$ , such that  $g : \mathbb{X} \rightarrow \mathbb{C}$ . The function  $g$  is referred to as the *observable function*. Let the space of observable functions be  $\mathcal{F} \subseteq C^0$ , where  $C^0$  denotes all continuous functions [35]. The Koopman operator,  $\mathcal{K}$ , is a linear, infinite-dimensional operator [36] that acts on  $g$  as follows:

$$\mathcal{K}g := g \circ \mathbf{F}, \quad (2)$$

where  $\circ$  denotes function composition, and thus:

$$\mathcal{K}g(\mathbf{x}[k]) = g(\mathbf{F}(\mathbf{x}[k-1])). \quad (3)$$

### B. Dynamic Mode Decomposition

For simplicity of notation, define

$$\mathbf{y}_k := g(\mathbf{x}[k]), \quad (4)$$

where  $\mathbf{y}_k \in \mathbb{R}^m$  is a vector of  $m$  measurements on (1) at time  $k$ . In some applications, the measurement set is the state itself, such that  $\mathbf{y}_k = \mathbf{x}_k$ , and  $m = n$ . In this paper, we consider the more general case defined in (4), where  $m \neq n$ .

Suppose that one collects sampled measurements of (1) at time instances  $k = \{0, 1, \dots, N\}$ . Define the data matrices

$$\mathbf{Y} := [\mathbf{y}_0 \ \mathbf{y}_1 \ \dots \ \mathbf{y}_{N-1}], \quad \mathbf{Y}' := [\mathbf{y}_1 \ \mathbf{y}_2 \ \dots \ \mathbf{y}_N], \quad (5)$$

where  $\mathbf{Y}, \mathbf{Y}' \in \mathbb{R}^{m \times N}$ . For a sufficiently large  $N$ , we get [33]

$$\mathbf{Y}' \approx \mathbf{A} \cdot \mathbf{Y}, \quad (6)$$

and  $\mathbf{A} \in \mathbb{R}^{m \times m}$  is a finite-dimensional approximation to the Koopman operator,  $\mathcal{K}$ . Note that in the original derivation of the DMD [3], [33],  $\mathbf{A}$  takes the form of a companion matrix. As discussed in [33], however, a practical implementation based on the companion matrix yields an ill-conditioned algorithm. Instead, the following procedure is suggested in [33]:

- 1) Compute a reduced singular value decomposition of  $\mathbf{Y}$ :

$$\mathbf{Y} = \mathbf{U} \mathbf{\Sigma} \mathbf{V}, \quad (7)$$

where  $\mathbf{U}$  is  $m \times c$ ,  $\mathbf{\Sigma}$  is diagonal and  $c \times c$ ,  $\mathbf{V}$  is  $N \times c$ , and  $c$  is the rank of  $\mathbf{Y}$ .

- 2) Then, compute

$$\tilde{\mathbf{A}} = \mathbf{U} \mathbf{Y} \mathbf{V} \mathbf{\Sigma}^{-1}. \quad (8)$$

The numerical procedure goes on with an eigendecomposition of  $\tilde{\mathbf{A}}$  but, for the purpose of this paper, the above outlined steps suffice. As explained in [33], (8) amounts to a projection of the linear operator  $\mathbf{A}$  onto a proper orthogonal decomposition basis. The method proposed in [33] is known as the standard DMD.

In addition to the standard DMD, the exact DMD proposed by Tu *et al.* [34] is widely used. It is as follows:

- 1) Let

$$\mathbf{Y}' = \mathbf{A} \cdot \mathbf{Y}. \quad (9)$$

- 2) Post-multiply both sides of (9) by  $\mathbf{Y}^\top$  to get

$$\mathbf{Y}' \mathbf{Y}^\top = \mathbf{A} \mathbf{Y} \mathbf{Y}^\top. \quad (10)$$

- 3) Then, an estimate of  $\mathbf{A}$  is obtained as

$$\hat{\mathbf{A}} = \mathbf{Y}' \mathbf{Y}^\top (\mathbf{Y} \mathbf{Y}^\top)^{-1}. \quad (11)$$

Note that  $\mathbf{Y}^\top (\mathbf{Y} \mathbf{Y}^\top)^{-1}$  in (11) is the Moore-Penrose inverse  $\mathbf{Y}^\dagger$  of a matrix  $\mathbf{Y}$ , and the matrix  $(\mathbf{Y} \mathbf{Y}^\top)$  is invertible as long as  $\mathbf{Y}$  has linearly independent rows. Given an estimate  $\hat{\mathbf{A}}$ , it is straightforward to compute the approximations to the Koopman eigenvalues and Koopman modes [4].

Now, let the residual (column) vector at time  $k$  be defined as

$$\mathbf{r}_k := \mathbf{y}_{k+1} - \mathbf{A} \mathbf{y}_k, \quad (12)$$

and let the  $i$ th element of  $\mathbf{r}_k$  be given by

$$r_k^{[i]} = y_{k+1}^{[i]} - \mathbf{a}_i^\top \mathbf{y}_k, \quad (13)$$

where  $\mathbf{a}_i^\top$  denotes the  $i$ th row of  $\mathbf{A}$ . It can be shown that (11) is the solution to a classic linear least-squares regression problem, that is,

$$\text{minimize} \quad \sum_{k=0}^{N-1} \sum_{i=1}^m \rho_{\ell s} \left( r_k^{[i]} \right), \quad (14)$$

where the least-squares loss function  $\rho_{\ell s} \left( r_k^{[i]} \right) = \frac{1}{2} \left( r_k^{[i]} \right)^2$ .

**Lemma 1.** *The estimate  $\hat{\mathbf{A}}$  in (11) is the least-squares solution to (6).*

*Proof.* Define

$$\begin{aligned} J_{\ell s}(\mathbf{a}_i) &:= \sum_{k=0}^{N-1} \sum_{i=1}^m \frac{1}{2} \left( y_{k+1}^{[i]} - \mathbf{a}_i^\top \mathbf{y}_k \right) \left( y_{k+1}^{[i]} - \mathbf{a}_i^\top \mathbf{y}_k \right) \quad (15) \\ &= \sum_{k=0}^{N-1} \sum_{i=1}^m \frac{1}{2} \left( r_k^{[i]} \right)^2 = \sum_{k=0}^{N-1} \sum_{i=1}^m \rho_{\ell s} \left( r_k^{[i]} \right). \end{aligned}$$

To minimize  $J_{\ell s}(\mathbf{a}_i)$ , one takes its partial derivative with respect to  $\mathbf{a}_i$  and sets it equal to zero. Formally, we have

$$\begin{aligned} \frac{\partial J_{\ell s}(\mathbf{a}_i)}{\partial \mathbf{a}_i} &= \sum_{k=0}^{N-1} \sum_{i=1}^m \frac{\partial \rho_{\ell s} \left( r_k^{[i]} \right)}{\partial r_k^{[i]}} \cdot \frac{\partial r_k^{[i]}}{\partial \mathbf{a}_i} \\ &= - \sum_{k=0}^{N-1} \sum_{i=1}^m \psi_{\ell s} \left( r_k^{[i]} \right) \mathbf{y}_k = \mathbf{0}_m, \quad (16) \end{aligned}$$

where  $\mathbf{0}_m$  denotes a column vector of dimension  $m$ , which has all elements equal to zero, and

$$\psi_{\ell s} \left( r_k^{[i]} \right) = r_k^{[i]} \quad (17)$$

is the least-squares  $\psi$ -function, also known as the score function. From (16), one has

$$\begin{aligned} \sum_{k=0}^{N-1} \mathbf{r}_k \mathbf{y}_k^\top &= \sum_{k=0}^{N-1} (\mathbf{y}_{k+1} - \mathbf{A} \mathbf{y}_k) \mathbf{y}_k^\top = \sum_{k=0}^{N-1} \mathbf{y}_{k+1} \mathbf{y}_k^\top - \mathbf{A} \mathbf{y}_k \mathbf{y}_k^\top \\ &= \mathbf{Y}' \mathbf{Y}^\top - \mathbf{A} \mathbf{Y} \mathbf{Y}^\top = \mathbf{0}_{mm}, \quad (18) \end{aligned}$$

where  $\mathbf{0}_{mm}$  denotes a square matrix of dimension  $m$ , which has all elements equal to zero. Finally, from (18), we have

$$\mathbf{A} = \mathbf{Y}' \mathbf{Y}^\top (\mathbf{Y} \mathbf{Y}^\top)^{-1}, \quad (19)$$

and the proof is complete.  $\square$

**Remark 1.** *In statistics, the score function is the gradient of the log-likelihood function with respect to the parameter vector. Evaluated at a particular point of the parameter vector, the score indicates the steepness of the log-likelihood function and thereby the sensitivity to infinitesimal changes to the parameter values. If the log-likelihood function is continuous over the parameter space, then the score will vanish at a local maximum or minimum; this fact is used in the maximum likelihood estimation to find the parameter values that maximize the likelihood function and, therefore, minimize the estimation residues.*

**Remark 2.** *To have a bounded influence function, which is proportional to the score function, is a necessary condition for a robust estimator. From (17), it is clear that the least-squares score function is unbounded and, therefore, the least-squares estimator is not robust.*

Hence, it is expected that a least-squares estimator provides strongly biased results when the samples contained in the

data matrices  $\mathbf{Y}$  and  $\mathbf{Y}'$  are contaminated with outliers. As a result, in the presence of outliers, the exact DMD has an unbounded bias. Moreover, it can be shown that singular value decomposition is also based on a least-squares estimator. Therefore, in the presence of outliers, the standard DMD has also an unbounded bias.

### III. ROBUST EXACT DYNAMIC MODE DECOMPOSITION

It is necessary to modify the exact DMD to construct a statistically robust DMD method. First, outliers must be detected and identified. To this end, we rely on projection statistics to derive weights over the interval  $[0, 1]$  that are used to bound the influence of outliers. Specifically, the farther an outlier is from the center of the data cloud, the smaller its assigned weight. All remaining data points not identified as outliers receive a weight equal to 1. These weights are incorporated into the Huber loss function to bound the influence of outliers in the estimation process. The details are presented next.

#### A. Multidimensional Outlier Detection

The detection and identification of outliers are key steps in robust statistics. In statistical analysis, several methods have been proposed to detect an outlier based on its distance from the majority of the data point cloud, as explained next.

Let an univariate data set  $\mathbb{P} \subseteq \mathbb{R}$  be  $\{p_1, \dots, p_N\}$ . A measure of the distance between a data point,  $p_k \in \mathbb{P}$ , and the center of the data cloud is given by  $\frac{p_k - \hat{\mu}}{\hat{s}}$ , where  $\hat{\mu}$  denotes an estimator of location, and  $\hat{s}$  denotes an estimator of scale. A classic measure of distance in the univariate case is provided by:

$$d(p_k) = \frac{p_k - \hat{\mu}_{\mathbb{P}}}{\hat{\sigma}_{\mathbb{P}}}, \quad (20)$$

where the sample mean of the data points in  $\mathbb{P}$ ,  $\hat{\mu}_{\mathbb{P}}$ , is used as an estimator of location; and the sample standard deviation of the data points in  $\mathbb{P}$ ,  $\hat{\sigma}_{\mathbb{P}}$ , is used as an estimator of scale;  $d(p_k)$  is often referred to as the z-score of the data point  $p_k$ . The classic measure of distance given by (20) is generalized to the multivariate case by the Mahalanobis distance.

**Definition 1** (Mahalanobis distance). *Let a multivariate data set  $\mathbb{P} \subseteq \mathbb{R}^m$  be  $\{\mathbf{p}_1, \dots, \mathbf{p}_N\}$ . The Mahalanobis distance between a data point,  $\mathbf{p}_k$ , and the data cloud composed by all data points in  $\mathbb{P}$  is defined as*

$$d_M(\mathbf{p}_k) := \left[ (\mathbf{p}_k - \hat{\boldsymbol{\mu}})^\top \hat{\mathbf{S}}^{-1} (\mathbf{p}_k - \hat{\boldsymbol{\mu}}) \right]^{1/2}, \quad (21)$$

where  $\hat{\boldsymbol{\mu}} = (\hat{\mu}_1, \dots, \hat{\mu}_N)^\top$  and  $\hat{\mathbf{S}}$  are, respectively, the sample mean and the sample covariance matrix of the data points in  $\mathbb{P}$ .

By comparing (20) and (21), note that the sample standard deviation used in the univariate case is replaced by the sample covariance matrix in the multivariate case.

It can be shown (see [16]) that for a scalar  $b \in \mathbb{R}$ , the set of data points for which  $d_M^2 < b$  lies inside an ellipsoid with the center at  $\hat{\boldsymbol{\mu}}$ . Moreover, if the data points in  $\mathbb{P} \subseteq \mathbb{R}^m$  follow a multivariate normal distribution, then the values of  $d_M^2$  follow a chi-square distribution with  $m$  degrees of freedom,  $\chi_m^2$ .

Hence, there is a probability of  $1 - \alpha$  that a data point  $\mathbf{p}_k$  such that  $d_M^2 \leq \chi_{m,1-\alpha}^2$  is located within an ellipsoid given by  $d_M^2 = \chi_{m,1-\alpha}^2$  that is centered at  $\hat{\boldsymbol{\mu}}$ . This provides the rationale used to tag outliers—that is, an outlier is any data point for which the Mahalanobis distance is larger than a threshold, e.g.,  $(\chi_{m,0.975}^2)^{1/2}$ . But because  $d_M$  is calculated via non-robust estimators of location and scale, it is vulnerable to the masking effect of multiple outliers, especially when the latter appear in clusters [37]. In other words, the corresponding ellipsoid is inflated to the point that it encompasses outliers, which can no longer be identified. To gain robustness, one can replace the sample mean and the sample covariance matrix in (21) by robust estimators of location and scale, respectively. This is discussed next.

**Definition 2** (Median absolute deviation from median in the case of an univariate data set). *Let a univariate data set,  $\mathbb{P} \subseteq \mathbb{R}$ , be  $\{p_1, \dots, p_N\}$ . A very robust estimator of scale [38] is the median absolute deviation from the median, which is defined as*

$$\text{mad}_{\mathbb{P}} := 1.4826 \cdot \text{median} |p_k - \text{median}(\mathbf{p}^T)|, \quad (22)$$

for  $k = \{1, \dots, N\}$ , where  $\mathbf{p}^T = [p_1 \ p_2 \ \dots \ p_N]$ , and the constant 1.4826 makes the estimator consistent at normal distributions.

In the univariate case, a robust distance between  $p_k$  and the center of the data cloud is given by:

$$d_r(p_k) = \frac{|p_k - \text{median}(\mathbf{p}^T)|}{\text{mad}_{\mathbb{P}}}. \quad (23)$$

**Definition 3** (Median absolute deviation from the median in the case of a multivariate data set). *Let a multivariate data set,  $\mathbb{P} \subseteq \mathbb{R}^m$ , be  $\{\mathbf{p}_1, \dots, \mathbf{p}_N\}$ . The median absolute deviation from the median is defined as:*

$$\hat{s}_1 := 1.4826 \cdot \text{median}_k (|\mathbf{p}_k^T \mathbf{v} - \text{median}_j (\mathbf{p}_j^T \mathbf{v})|), \quad (24)$$

for  $k, j = \{1, 2, \dots, N\}$ , where  $\mathbf{v}$  is the direction to which the data points are projected.

In the multivariate case, however, it is challenging to align all multivariate data points such that a meaningful measure of distance can be obtained. A solution to this challenge followed the realization that the Mahalanobis distance can be written as follows [39]:

$$\begin{aligned} d_M(\mathbf{p}_k) &= \left[ (\mathbf{p}_k - \hat{\boldsymbol{\mu}})^T \hat{\mathbf{S}}^{-1} (\mathbf{p}_k - \hat{\boldsymbol{\mu}}) \right]^{1/2} \\ &\equiv \max_{|\mathbf{v}|=1} \left( \frac{|\mathbf{p}_k^T \mathbf{v} - \hat{\ell}(\mathbf{p}_1^T \mathbf{v}, \dots, \mathbf{p}_N^T \mathbf{v})|}{\hat{s}(\mathbf{p}_1^T \mathbf{v}, \dots, \mathbf{p}_N^T \mathbf{v})} \right), \end{aligned} \quad (25)$$

where  $\hat{\ell}$  and  $\hat{s}$  denote, respectively, an estimator of location and scale. Note that the maximization should be considered on all possible directions  $\mathbf{v}$ . To robustify (25), Donoho and Gasko [40] suggest using the sample median as the estimator of location and the median absolute deviation from the median given by (24),  $\hat{s}_1$ , as the estimator of scale. This distance is referred to as the *projection statistic*, and it is defined as

$$d_{\text{ps}}(\mathbf{p}_k) = d_{\text{ps},k} := \max_{|\mathbf{v}|=1} \left( \frac{|\mathbf{p}_k^T \mathbf{v} - \text{median}_j (\mathbf{p}_j^T \mathbf{v})|}{\hat{s}_1} \right), \quad (26)$$

where the sample median and  $\hat{s}_1$  are calculated on the direction of all feasible unit vectors  $\mathbf{v}$ . Unfortunately,  $\hat{s}_1$  loses statistical efficiency for asymmetric distributions. To address this issue, Croux and Rousseeuw [38], [41] propose another robust estimator of scale, which is statistically efficient for asymmetric distributions, and it is defined as

$$\hat{s}_2 := 1.1926 \cdot \text{lomed}_k ( \text{lomed}_{j \neq k} |\mathbf{p}_k^T \mathbf{v} - \mathbf{p}_j^T \mathbf{v}| ), \quad (27)$$

for  $k, j = \{1, \dots, N\}$ , where *lomed* denotes a low median—that is, the  $((N+1)/2)$ -th order statistic out of  $N$  data points. Eq. (27) reads as follows: for each  $k$ , we compute the low median of  $|\mathbf{p}_k - \mathbf{p}_j|$  for  $j = \{1, \dots, N\}$ . This yields  $N$  data points, the low median of which gives the final estimate,  $\hat{s}_2$ . The factor 1.1926 is for consistency at the normal distribution.

Yet, another challenge encountered in calculating projection statistics lies in the fact that considering all possible directions of  $\mathbf{v}$  cannot be realized. To address this, Gasko and Donoho [42] suggest considering only the directions that originate from the coordinate-wise median vector,  $\mathbf{v}_{\text{med}}$ , and that pass through each data point  $\mathbf{p}_k$ , yielding

$$\mathbf{v}_k = \mathbf{p}_k - \mathbf{v}_{\text{med}}, \quad (28)$$

where

$$\mathbf{v}_{\text{med}} = [\text{median}_j(\mathbf{x}_{j1}) \ \text{median}_j(\mathbf{x}_{j2}) \ \dots \ \text{median}_j(\mathbf{x}_{jm})]^T. \quad (29)$$

Thus, it is enough to investigate  $m$  directions. Moreover, it is not necessary to consider  $\mathbf{v}$  to be of unit length because  $\hat{s}_1$  and  $\hat{s}_2$  are affine-equivariant scale estimators.

As it is the case for the Mahalanobis distance, the projected statistics approximately follow a chi-square distribution with  $m$  degrees of freedom when the data points follow a multivariate normal distribution [16]. Hence, the projection statistic of each data point,  $\mathbf{p}_k$ , is calculated, and if they exceed a threshold, e.g.,  $d_{\text{ps},k}^2 > \chi_{2,0.975}^2$ , then the associated data point is tagged as an outlier.

Note that in this paper, the data points  $\mathbf{p}_k$  are the columns of the data matrices given by (5).

Next, we develop a mechanism to suppress the adverse effect of the outliers on the estimation process. This is achieved by defining weights, which are calculated via projection statistics and incorporated into the Huber loss function.

#### B. Generalized Maximum-Likelihood Robust Estimation

**Definition 4** (Huber loss function). *The Huber loss function is defined as*

$$\rho_H(r_k^{[i]}) := \begin{cases} \frac{1}{2} (r_k^{[i]})^2 & \text{for } |r_k^{[i]}| \leq \delta, \\ \delta |r_k^{[i]}| - \frac{1}{2} \delta^2 & \text{otherwise.} \end{cases} \quad (30)$$

Note that  $\rho_H(\cdot)$  is quadratic for  $|r_k^{[i]}| \leq \delta$ , and linear otherwise. The quadratic and linear sections connect at the point where  $|r_k^{[i]}|$  is equal to the scalar-valued parameter  $\delta$ , which dictates the slope of the function. The parameter  $\delta$  is usually adjusted to have a numerical value between 1 and 3 to have high statistical efficiency at the normal distribution [16]. In this work, we set  $\delta = 1.5$ .

Now, let the SHGM estimator be defined such that it minimizes a convex objective function given by

$$J_H(\mathbf{a}_i) = \sum_{k=0}^{N-1} \sum_{i=1}^m w_k^2 \cdot \rho_H(r_{ks}^{[i]}), \quad (31)$$

where

$$r_{ks}^{[i]} = \frac{r_k^{[i]}}{s \cdot w_k} = \frac{1}{s \cdot w_k} (y_{k+1}^{[i]} - \mathbf{a}_i^T \mathbf{y}_k), \quad (32)$$

$$s = 1.4826 \cdot b_m \cdot \text{median} |\mathbf{r}_k^T|, \quad (33)$$

$$w_k = \min \left( 1, \frac{b}{d_{ps,k}^2} \right). \quad (34)$$

Here  $s$  is a robust estimator of scale,  $b_m$  is a correction factor,  $b$  is set equal to 1.5 for best statistical efficiency and to avoid large biases [16], and  $w_i$  are weights determined via projection statistics. The calculated weights play an essential role in the development of the RDMD method.

Having introduced a robust outlier detection algorithm and a generalized maximum-likelihood estimator that can suppress the bias introduced by the outliers, we are now in position to present the main result of this paper.

### C. Robust Dynamic Mode Decomposition

Let  $\mathbf{y}' = \text{col}(\mathbf{Y}') = [\mathbf{y}_1^T \dots \mathbf{y}_N^T]^T$ ,  $\mathbf{a} = \text{row}(\mathbf{A}) = [\mathbf{a}_1^T \dots \mathbf{a}_m^T]^T$ , and  $\mathbf{B} = \mathbf{I}_m \otimes \mathbf{Y}^T$ , where  $\mathbf{I}_m$  denotes an identity matrix of dimension  $m$ , and  $\otimes$  denotes the Kronecker product. The linear regression (9) can be rewritten as:

$$\begin{aligned} \mathbf{y}' &= \mathbf{B}\mathbf{a} = (\mathbf{I}_m \otimes \mathbf{Y}^T) \mathbf{a} \\ &= \begin{bmatrix} \mathbf{Y}^T & & & \\ & \mathbf{Y}^T & & \\ & & \ddots & \\ & & & \mathbf{Y}^T \end{bmatrix} \begin{bmatrix} \mathbf{a}_1 \\ \mathbf{a}_2 \\ \vdots \\ \mathbf{a}_m \end{bmatrix}. \end{aligned} \quad (35)$$

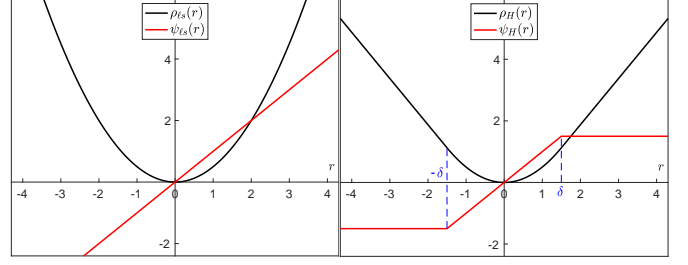
A solution to (35) can be found by solving  $m$  subproblems of the form:

$$\mathbf{y}' = \mathbf{Y}^T \mathbf{a}_i, \quad i = \{1, 2, \dots, m\}. \quad (36)$$

Hence, for each subproblem  $i$ , we seek a robust estimate,  $\hat{\mathbf{a}}_i$ , that is the solution to  $\mathbf{y}' = \mathbf{Y}^T \mathbf{a}_i$ . Note that the residues,  $r_k^{[i]}$ , given by (13) naturally apply to each subproblem  $i$ . Following (31), for each subproblem  $i$ :

$$J_H(\mathbf{a}_i) = \sum_{k=0}^{N-1} w_k^2 \cdot \rho_H(r_{ks}^{[i]}), \quad (37)$$

and the optimal solution to (37) is given by



(a) Least-squares loss/score function (b) Huber loss/score function

Fig. 1. Comparison between (a) least-squares estimator and (b) generalized maximum-likelihood robust estimator based on the Huber loss function.

$$\frac{\partial J_H(\mathbf{a}_i)}{\partial \mathbf{a}_i} = \sum_{k=0}^{N-1} -\frac{w_k \mathbf{y}_k}{s} \cdot \psi_H(r_{ks}^{[i]}) = \mathbf{0}_m, \quad (38)$$

where  $\psi_H(r_{ks}^{[i]}) = \partial \rho(r_{ks}^{[i]}) / r_{ks}^{[i]}$ , and

$$\psi_H(r_{ks}^{[i]}) = \begin{cases} r_{ks}^{[i]} & \text{for } |r_{ks}^{[i]}| \leq \delta, \\ \delta \cdot \text{sign}(r_{ks}^{[i]}) & \text{otherwise,} \end{cases} \quad (39)$$

is the Huber score function. An illustration of the least-squares and the Huber loss and score functions is shown in Fig. 1. We stress that having a bounded score function is a necessary condition for an estimator to be robust. Finally, a robust solution to (35) is given by solving (38) for  $i = \{1, 2, \dots, m\}$ , as follows. By multiplying and dividing the Huber score function in (38) by  $r_{ks}^{[i]}$ , and by defining the scalar weight function as  $q(r_{ks}^{[i]}) := \psi_H(r_{ks}^{[i]}) / r_{ks}^{[i]}$ , (38) can be expressed in matrix form, as follows:

$$\mathbf{Y}\mathbf{Q}(\mathbf{y}' - \mathbf{Y}^T \hat{\mathbf{a}}_i) = \mathbf{0}, \quad (40)$$

where  $\mathbf{Q} = \text{diag}(q(r_{ks}^{[i]}))$ . Solving for the estimate  $\hat{\mathbf{a}}_i$  using the iteratively reweighted least squares (IRLS) algorithm yields

$$\hat{\mathbf{a}}_i^{(v+1)} = (\mathbf{Y}\mathbf{Q}^{(v)}\mathbf{Y}^T)^{-1} \mathbf{Y}\mathbf{Q}^{(v)}\mathbf{y}', \quad (41)$$

where the superscript  $(v)$  indicates the  $v$ -th iteration. The condition for convergence of the IRLS algorithm is adjusted to meet  $\|\hat{\mathbf{a}}_i^{(v+1)} - \hat{\mathbf{a}}_i^{(v)}\| \leq 0.01$ . In what follows, the numerical method in (35)–(41) is referred to as K-RDMD, an allusion to the Kronecker product in (35). The computation time of K-RDMD is expected to increase substantially as the number of time instances  $N$  increases. This is addressed next.

Let us redefine the objective function as follows:

$$J_H(\mathbf{A}) = \sum_{k=1}^{N-1} w_k^2 \cdot \rho_H(\mathbf{r}_{ks}), \quad (42)$$

where  $\rho_H(\mathbf{r}_{ks})$  is a modified Huber loss function, as follows:

$$\rho_H(\mathbf{r}_{ks}) = \begin{cases} \frac{1}{2} \|\mathbf{r}_{ks}\|^2 & \text{for } \|\mathbf{r}_{ks}\| \leq \delta, \\ \delta \cdot \|\mathbf{r}_{ks}\| - \frac{1}{2} \delta^2 & \text{otherwise,} \end{cases} \quad (43)$$

where  $\mathbf{r}_{ks} = \mathbf{r}_k / (s \cdot w_k)$ ;  $\mathbf{r}_k$  and  $\delta$  are as defined before. The optimal solution to (42) is given by

$$\frac{\partial J_H(\mathbf{A})}{\partial \mathbf{A}} = \sum_{k=0}^{N-1} w_k^2 \cdot \frac{\partial \rho_H(\mathbf{r}_{ks})}{\partial \|\mathbf{r}_{ks}\|^2} \cdot \frac{\partial \|\mathbf{r}_{ks}\|^2}{\partial \|\mathbf{r}_k\|^2} \cdot \frac{\partial \|\mathbf{r}_k\|^2}{\partial \mathbf{A}}, \quad (44)$$

where

$$\frac{\partial \rho_H(\|\mathbf{r}_{ks}\|)}{\partial \|\mathbf{r}_{ks}\|^2} = \frac{1}{2\|\mathbf{r}_{ks}\|} \frac{\partial \rho_H(\|\mathbf{r}_{ks}\|)}{\partial \|\mathbf{r}_{ks}\|} = \frac{\psi_H(\|\mathbf{r}_{ks}\|)}{2\|\mathbf{r}_{ks}\|}, \quad (45)$$

$$\frac{\partial \|\mathbf{r}_{ks}\|^2}{\partial \|\mathbf{r}_k\|^2} = \frac{1}{s^2 w_k^2}, \quad (46)$$

$$\frac{\partial \|\mathbf{r}_k\|^2}{\partial \mathbf{A}} = 2\mathbf{r}_k \mathbf{y}_k^\top. \quad (47)$$

Thus, we have

$$\frac{\partial J_H(\mathbf{A})}{\partial \mathbf{A}} = \sum_{k=0}^{N-1} w_k^2 \frac{\psi_H(\|\mathbf{r}_{ks}\|)}{\|\mathbf{r}_{ks}\|} \frac{(\mathbf{y}_{k+1} - \mathbf{A}\mathbf{y}_k) \mathbf{y}_k^\top}{s^2 w_k^2} = \mathbf{0}. \quad (48)$$

By putting (48) in matrix form, we get

$$\mathbf{Y}\mathbf{Q}(\mathbf{Y}' - \mathbf{A}\mathbf{Y})^\top = \mathbf{0}, \quad (49)$$

where  $\mathbf{Q} = \text{diag}(\psi_H(\|\mathbf{r}_{ks}\|)/\|\mathbf{r}_{ks}\|)$ . Solving for the estimate  $\hat{\mathbf{A}}$  using the IRLS algorithm yields

$$\hat{\mathbf{A}}^{(v+1)} = \mathbf{Y}'\mathbf{Q}^{(v)}\mathbf{Y}^\top \left( \mathbf{Y}\mathbf{Q}^{(v)}\mathbf{Y}^\top \right)^{-1}. \quad (50)$$

The condition for convergence of the IRLS algorithm is set to meet  $\|\hat{\mathbf{A}}^{(v+1)} - \hat{\mathbf{A}}^{(v)}\|_F \leq 0.01$ . In what follows, the numerical method in (42)–(50) is referred to as N-RDMD, an allusion to the use of the norm of a residual vector. The performance of the proposed RDMD methods—K-RDMD and N-RDMD—is assessed in Section IV.

#### D. Robust Standard Dynamic Mode Decomposition

The first steps of the standard DMD are outlined in Section II-B, where  $c$  denotes the rank of  $\mathbf{Y}$ . Note that it is common to assume  $c \leq m < N$  for large data sets. Moreover, particularly for model order reduction, one is interested in a projection  $\tilde{\mathbf{A}} \in \mathbb{R}^{c' \times c'}$ , where  $c' < c$ . In this case, one disregards  $(c - c')$  nonzero elements of  $\Sigma$  and  $(c - c')$  columns of  $\mathbf{U}$  and  $\mathbf{V}$ . This changes the unitary property of  $\mathbf{U}$  and  $\mathbf{V}$  as follows:

$$\mathbf{U}^* \mathbf{U} = \mathbf{I}_{c'}, \quad \mathbf{U} \mathbf{U}^* \neq \mathbf{I}_N, \quad (51)$$

$$\mathbf{V}^* \mathbf{V} = \mathbf{I}_{c'}, \quad \mathbf{V} \mathbf{V}^* \neq \mathbf{I}_m. \quad (52)$$

In this section, we discuss how to robustify the standard DMD, even for the most challenging case described above. Let  $\mathbf{A} = \mathbf{T}\tilde{\mathbf{A}}\mathbf{T}^\dagger$ . Further, let  $\mathbf{T} \in \mathbb{C}^{N \times c'}$ , such that  $\mathbf{T}^\dagger \mathbf{T} = \mathbf{I}_{c'}$ . Then, the eigenvalues of  $\tilde{\mathbf{A}}$  are a subset of the eigenvalues of  $\mathbf{A}$ . Hence, for a known transformation  $\mathbf{T}$ , the residues in (12) can be rewritten as

$$\mathbf{r}_k = \mathbf{y}_{k+1} - \mathbf{T}\tilde{\mathbf{A}}\mathbf{T}^\dagger \mathbf{y}_k. \quad (53)$$

Thus, we have

$$\mathbf{T}^\dagger \mathbf{Y}\mathbf{Q} \left( \mathbf{T}^\dagger \mathbf{Y}' - \tilde{\mathbf{A}}\mathbf{T}^\dagger \mathbf{Y} \right)^\top = \mathbf{0}, \quad (54)$$

yielding to the iterative formula given by

$$\tilde{\mathbf{A}}^{(v+1)} = \mathbf{T}^\dagger \mathbf{Y}'\mathbf{Q}^{(v)}\mathbf{Y}^\top \mathbf{T} \left( \mathbf{T}^\dagger \mathbf{Y}\mathbf{Q}^{(v)}\mathbf{Y}^\top \mathbf{T} \right)^{-1}. \quad (55)$$

Note that in (55), the weights calculated via projection statistics act on the matrix  $\mathbf{Q}$ . Also note that if  $\mathbf{T}\mathbf{T}^\dagger = \mathbf{I}_N$ , then  $\mathbf{Q}$  is canceled out from (55), leading to an ordinary least-squares solution  $\tilde{\mathbf{A}} = \mathbf{Y}'\mathbf{Y}^\dagger$ , and we lose the robustness; therefore, to guarantee the robustness, we should have  $\mathbf{T}\mathbf{T}^\dagger \neq \mathbf{I}_N$ . To relax such a constraint on (55), one might resort to the following iterative procedure:

$$\tilde{\mathbf{A}}^{(v+1)} = \mathbf{T}^\dagger \mathbf{Y}'\mathbf{Q}^{(v)}\mathbf{Y}^\top \mathbf{T} \left( \mathbf{T}^\dagger \mathbf{Y}\mathbf{Q}^{(v)}\mathbf{Y}^\top \mathbf{T} + \gamma^2 \mathbf{I} \right)^{-1}, \quad (56)$$

This is known as the Tikhonov regularization, which is usually used to solve ill-posed regression problems [43]. In (56),  $\gamma$  is a small positive constant. It also can avoid possible numerical problems in calculating the inverse in (55).

Although the estimation of  $\tilde{\mathbf{A}}$  from (55) is robust to outliers, it is not guaranteed that it includes all the dominant modes in the data. In other words, although each eigenvalue of  $\tilde{\mathbf{A}}$  is also an eigenvalue of the original  $\mathbf{A}$ , there is the possibility that the dominant eigenvalues are not included. This is mainly determined by how one selects the reduction matrix  $\mathbf{T}$ . An option is to choose  $\mathbf{T} = \mathbf{U}$ , as is done for the standard DMD. Note that as previously explained,  $\mathbf{U}$  is not a unitary matrix; therefore, robustness is ensured. On the other hand, because there are outliers in the data matrix  $\mathbf{Y}$ , such a reduction might not be able to cover all dominant modes. It is observed that for a low percentage of outliers among the data points, this selection captures the dominant eigenvalues. Another option is to preprocess the data matrices before performing the singular value decomposition. A comprehensive investigation on the choice of the similarity transformation in the RDMD is a topic for future research.

## IV. SIMULATION RESULTS

In what follows, the performance of the proposed RDMD is assessed by using a variety of canonical dynamical systems. Further, the performance of the proposed RDMD is compared to the performance of

- the exact DMD proposed in [34];
- the total DMD (TDMD) proposed in [22];
- the optimization-based DMD (ODMD) proposed in [24];
- the robust trimmed DMD proposed in [25].

We start by comparing the performance of the two variations of the RDMD developed in Section III-C.

#### A. Comparison between K-RDMD and N-RDMD

Consider a network of  $s$  oscillators connected in a ring topology. The differential equation describing the angular displacement of the  $k$ -th oscillator is given by

$$\ddot{\theta}_k + \ell_k^T \theta + d_k \theta_k = 0, \quad (57)$$

where  $\theta_k$  and  $d_k$  are, respectively, the angle and the damping coefficient of the  $k$ -th oscillator;  $\ell_k^T$  denotes the  $k$ -th row of the Laplacian matrix  $\mathcal{L}$ ; and  $\theta = [\theta_1 \ \theta_2 \ \dots \ \theta_s]^T$ . Here, a ring topology with  $s = 15$  oscillators is considered. Note that the number of states is  $m = 2s$ . The state-space equations are written as

$$\begin{aligned} \dot{\theta} &= \omega, \\ \dot{\omega} &= -\mathcal{L}\theta - D\theta, \end{aligned} \quad (58)$$

$\omega = [\omega_1 \ \dots \ \omega_s]^T$ , and  $D = \text{diag}(d_1, \dots, d_s)$ . The data sampled are collected with sample time 0.01 second. The damping  $d_k$  is set to 0.05 for all  $k$ .

We observe that N-RDMD yields larger cumulative errors when the number of snapshots  $N$  is small. See Table I. This is because N-RDMD encapsulates all the information contained in the residual vector by taking its norm. As a consequence, in the presence of outliers, an entire snapshot is down-weighted. Hence, though the N-RDMD successfully suppresses the adverse effect of the outliers in the estimation process, it also disregards some good information. For small  $N$ , this might lead to the loss of statistical efficiency. Conversely, K-RDMD treats every residue within the residual vector individually and, thus, maintains good statistical efficiency even for small  $N$ . For a large number of snapshots  $N$ , however, N-RDMD offers a computational advantage. This is to be expected because K-RDMD has to solve  $m$  subproblems of dimension  $N$ , whereas N-RDMD solves a single problem of dimension  $N$ . Fig. 2 shows the performance of N-RDMD and K-RDMD for the network of the coupled oscillators with 15 oscillators and 500 snapshots. We observe that both are robust to outliers. The reconstruction cumulative error that is defined as  $\sum_{i=0}^k \|\mathbf{x}_{i,\text{reconstructed}} - \mathbf{x}_{i,\text{true}}\|$  is also depicted in Fig. 2. A difference in performance is observed in the reconstruction of a state variable, i.e., the N-RDMD performs better than the K-RDMD in reconstructing the state value. This difference is further investigated under three different scenarios, which are summarized in Table I. One can expect that despite the high computational effort by K-RDMD, it performs better than N-RDMD; however, note that the K-RDMD solves  $m = 2s$  separate robust estimation problems to solve for each row of the matrix  $\mathbf{A}$  using the IRLS algorithm. Note that each IRLS loop has an error threshold that overall leads to a larger error in estimating the matrix  $\mathbf{A}$ , whereas the N-RDMD uses a single IRLS loop using the Frobenius norm of the error matrix.

In what follows, the performance of N-RDMD is compared to other DMD methods available in the literature, where it will be referred to as RDMD. We choose N-RDMD because it has a higher computational efficiency than K-RDMD. We start by presenting results on a simple linear dynamical system and gradually move toward more complex nonlinear dynamical systems.

### B. Linear System

Consider the linear dynamical system:

$$\begin{aligned} \dot{x}_1 &= -x_1 - 3x_2, \\ \dot{x}_2 &= x_1 + x_2. \end{aligned} \quad (59)$$

TABLE I  
COMPUTATION TIME (S) AND CUMULATIVE ERROR OF K-RDMD AND N-RDMD

| Problem dimension |        | $s = 15,$<br>$N = 500$ | $s = 150,$<br>$N = 40$ | $s = 200,$<br>$N = 500$ |
|-------------------|--------|------------------------|------------------------|-------------------------|
| Cumulative error  | N-RDMD | 3.4815                 | 15.9835                | 9.8851                  |
|                   | K-RDMD | 12.6921                | 10.1266                | 44.7982                 |
| Computation time  | N-RDMD | 3.0784                 | 0.0527                 | 8.2187                  |
|                   | K-RDMD | 3.1158                 | 0.5613                 | 44.7982                 |

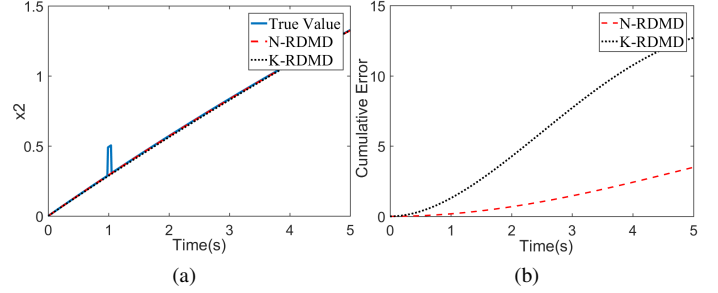


Fig. 2. Ring network defined in (58) with  $s = 15$  oscillators and  $N = 500$  snapshots. (a) Reconstruction of the angular velocity of the first oscillator in the presence of outliers of magnitude 0.2 from  $t = 1$  to  $t = 1.05$  seconds. (b) Cumulative error of the state reconstruction.

TABLE II  
EIGENVALUES OF (59) CALCULATED USING VARIOUS METHODS UNDER THREE DIFFERENT SCENARIOS

|            | Outlier-free case    | Case 2                | Case 3                |
|------------|----------------------|-----------------------|-----------------------|
| True value | $0.000 \pm j1.4142$  | $0.000 \pm j1.4142$   | $0.000 \pm j1.4142$   |
| DMD [33]   | $0.0000 \pm j1.4142$ | $-0.1747 \pm j1.3787$ | $-0.3574 \pm j1.3115$ |
| TDMD [22]  | $0.0000 \pm j1.4142$ | $-0.0021 \pm j1.4041$ | $-0.0063 \pm j1.3643$ |
| ODMD [24]  | $0.0000 \pm j1.4142$ | $-0.2626 \pm j1.3669$ | $-0.4834 \pm j1.2817$ |
| N-RDMD     | $0.0013 \pm j1.4142$ | $-0.0027 \pm j1.4131$ | $-0.0043 \pm j1.4126$ |

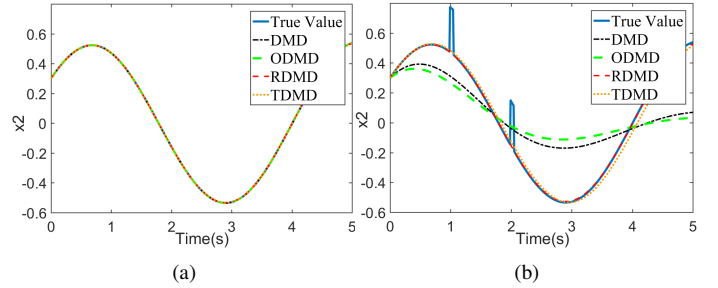


Fig. 3. Reconstruction of  $x_2$  for the linear system in (59). (a) Outlier-free case. (b) Case with outliers of magnitude 0.3 from  $t = 1$  to  $t = 1.05$  seconds and from  $t = 2$  to  $t = 2.05$  seconds.

We investigate three cases as follows:

- 1) the sampled data is free of outliers;
- 2) the sampled data is contaminated with outliers of magnitude 0.3 from  $t = 1$  to  $t = 1.05$  seconds;
- 3) the sampled data is contaminated with outliers of magnitude 0.3 from  $t = 1$  to  $t = 1.05$  seconds and from  $t = 2$  to  $t = 2.05$  seconds.

Table II shows the eigenvalues of  $\hat{\mathbf{A}}$  computed for each case. Further, the reconstruction of  $x_2$  in cases 1 and 3 is depicted



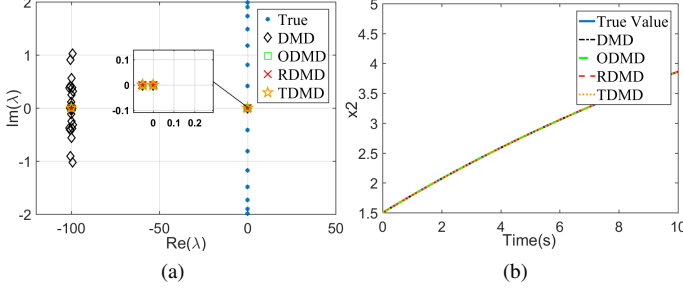


Fig. 4. Network of coupled oscillators when the sampled data are outlier free. (a) Eigenvalues. (b) Reconstruction of state  $x_2$ .

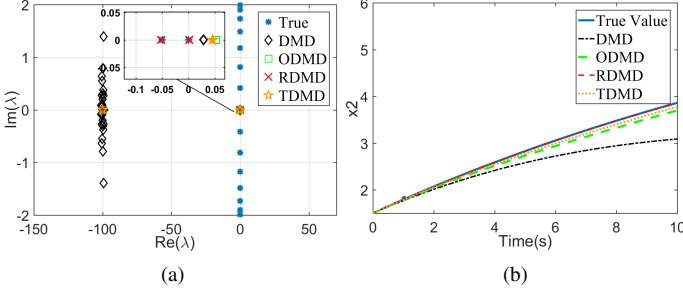


Fig. 5. Network of coupled oscillators when the sampled data are contaminated with outliers of magnitude 0.1 between  $t = 1$  and  $t = 1.05$  seconds. (a) Eigenvalues. (b) Reconstruction of state  $x_2$ .

in Fig. 3. We observe in Table II that the accuracy of the RDMD is slightly less than that of other DMD methods in the outlier-free case. As discussed in previous sections, the RDMD presents high statistical efficiency under ideal scenarios while being robust to deviations from assumptions about the data. Indeed, we observe that RDMD performs best for higher percentages of outliers.

### C. Network of Coupled Oscillators

Next, we consider the network of coupled oscillators defined in (58). Figs. 4 and 5 show the performance of the considered DMD methods. We observe in Fig. 4 that all methods capture the dominant eigenvalue of the system in an ideal case without outliers. Further, all methods yield an accurate reconstruction of state  $x_2 = \omega_2$ . Conversely, in Fig. 5, we see that N-RDMD performs best when the sampled data are contaminated with outliers of magnitude 0.1 between  $t = 1$  and  $t = 1.05$  seconds.

### D. Slow-Manifold System

Now, consider a slow-manifold system given by

$$\begin{aligned} \dot{x}_1 &= \mu x_1, \\ \dot{x}_2 &= \lambda (x_2 - \rho(x_1)), \end{aligned} \quad (60)$$

with  $\mu = -0.05$ ,  $\lambda = -1$ , and  $\rho(x_1) = x_1^2$ . In (60), the slow dynamics is dictated by the eigenvalue equal to  $-0.05$ , whereas the second state  $x_2$  quickly approaches the manifold  $x_2 = \rho(x_1)$ . In this case, we simulate a case where the sampled data are contaminated with outliers of magnitude 0.2 between

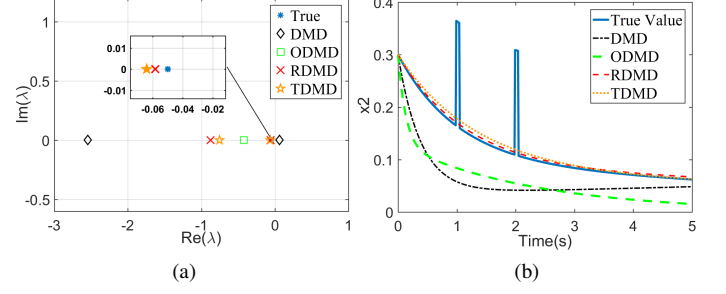


Fig. 6. Slow-manifold system when the sampled data are contaminated with outliers of magnitude 0.2 between  $t = 1$  and  $t = 1.05$  seconds and between  $t = 2$  and  $t = 2.05$  seconds. (a) Eigenvalues. (b) Reconstruction of state  $x_2$ .

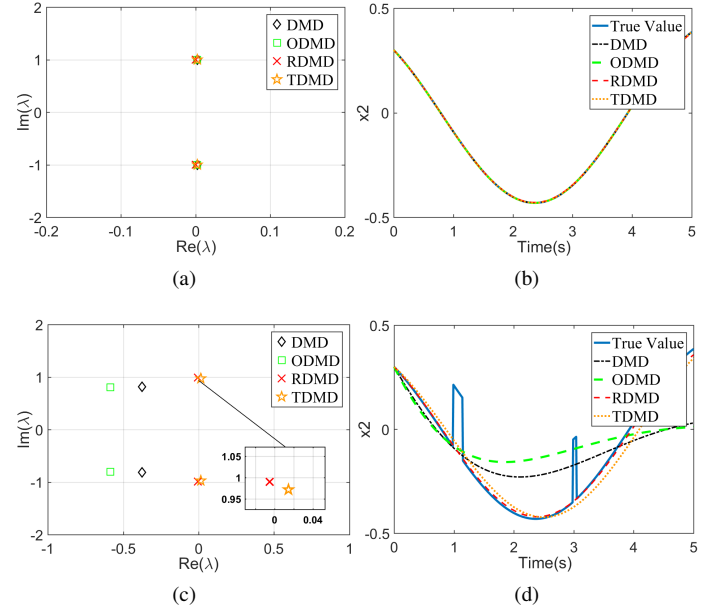


Fig. 7. Estimated eigenvalues and reconstruction of state  $x_2$  for the Van der Pol oscillator in (61). (a), (b) Outlier-free data. (c), (d) Sampled data contaminated with outliers of magnitude 0.3 from  $t = 1$  to  $t = 1.15$  seconds and from  $t = 3$  to  $t = 3.05$  seconds.

$t = 1$  and  $t = 1.05$  seconds and between  $t = 2$  and  $t = 2.05$  seconds. Fig. 6 depicts the estimated eigenvalues. We observe that N-RDMD performs best in capturing the eigenvalue equal to  $-0.05$  and that corresponds to the slow dynamics.

### E. Van der Pol Oscillator

Finally, we consider the Van der Pol oscillator given by

$$\begin{aligned} \dot{x}_1 &= x_2, \\ \dot{x}_2 &= \mu (1 - x_1^2) x_2, \end{aligned} \quad (61)$$

and the results are shown in Fig. 7. Note that for data collected from nonlinearly evolving signals, the approximated DMD modes are reflecting the behavior of the most dominant Koopman modes. As shown in Fig. 7, when there is no outlier contamination within the data set, all considered DMD methods calculate approximately the same dominant eigenvalues, and a good response of  $x_2$  is reconstructed; however, when



there are some outliers among the data set, only N-RDMD can capture the same eigenvalues as found for the outlier-free data. In other words, the process of finding eigenvalues has been made robust against outliers.

#### F. Dynamic Mode Decomposition of Large Data Sets

Next, we assess the performance of N-RDMD for larger data sets. First, we consider a random linear system of the form given by

$$\dot{\mathbf{x}}(t) = \Theta \mathbf{x}(t), \quad (62)$$

where  $\Theta$  is a random matrix of the form  $\text{randn}(m, m) - h\mathbf{I}_m$ , and  $h$  is chosen such that all eigenvalues reside in the left half of the complex Cartesian plane. The data are collected for  $N = 200$  time samples. The order of the truncated dynamics is considered to be  $c' = 25$  for all the simulated DMD methods. Note that ODMD [24] is not included in this case because no solution can be attained. We observe in Fig. 8 that the exact DMD and TDMD perform best when the data are outlier free; however, N-RDMD outperforms other methods when the data are contaminated with outliers. Note that TDMD estimates eigenvalues with the positive real part, which yields unstable dynamics; therefore, we do not plot the TDMD response in Fig. 8(d).

As a second example, consider a generalized representation of a slow-manifold nonlinear system given by

$$\begin{aligned} \dot{\mathbf{x}}_1 &= \mathbf{W} \mathbf{x}_1, \\ \dot{\mathbf{x}}_2 &= \Lambda (\mathbf{x}_2 - \mathbf{P}(\mathbf{x}_1)), \end{aligned} \quad (63)$$

where  $\mathbf{x}_1, \mathbf{x}_2 \in \mathbb{R}^{m/2}$ ,  $\mathbf{W} = \text{diag}(\mu_1, \dots, \mu_{m/2})$ ,  $\Lambda = \text{diag}(\lambda_1, \dots, \lambda_{m/2})$ ,  $\mu_i < 0$ ,  $\lambda_i > 0$ ,  $i = \{1, \dots, m/2\}$ , and  $\mathbf{P}(\mathbf{x}_1) = [\mathbf{P}_1(\mathbf{x}_1) \dots \mathbf{P}_{m/2}(\mathbf{x}_1)]^T$ . Here, we choose  $\mu_i$  as negative random numbers,  $\Lambda = \mathbf{I}_{m/2}$ ,  $\mathbf{P}_i(\mathbf{x}_1) = \left(\sum_{j=1}^{m/2} \mathbf{x}_{1j}\right)^2$ , and  $m = 500$ .

The results shown in Fig. 9 demonstrate the ability of all DMD methods in capturing the dominant eigenvalues, located at  $\mu_i$ , and in reconstructing state  $x_2$  when the data are outlier free. Further, as shown in Fig. 9, N-RDMD outperforms DMD and TDMD when the sampled data are contaminated with outliers of magnitude 0.1 from  $t = 1$  to  $t = 1.05$  seconds.

#### G. Computation Time

A comparison of the computation time for all DMD methods applied on the examples in sections IV-B to IV-F is given in Table II. Compared to other methods, N-RDMD has a higher computation time, the vast majority of which is spent computing projection statistics. This is essentially the price paid for statistical robustness.

#### H. Gaussian and Non-Gaussian Noises

The proposed RDMD has two important practical advantages: i) it can suppress the adverse effect of outliers, and ii) it is statistically efficient even if the residues do not follow a Gaussian distribution; see, e.g., [32], [44], [45]. In this section,

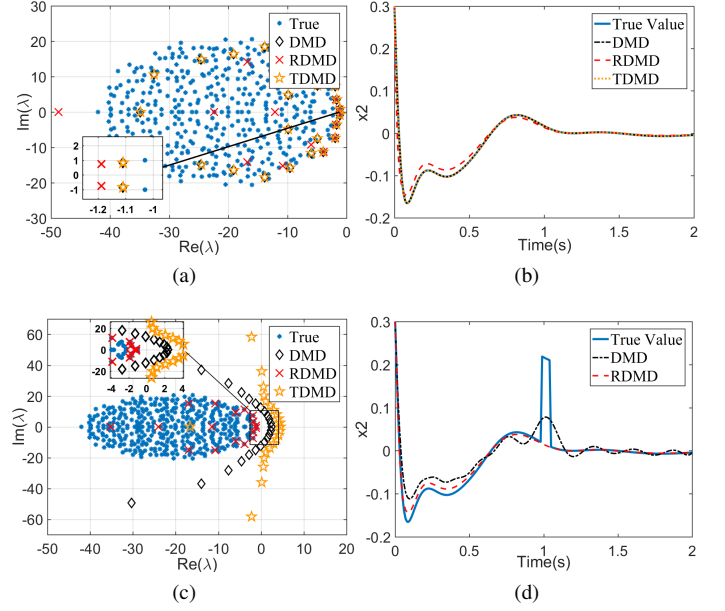


Fig. 8. Estimated eigenvalues and reconstruction of state  $x_2$  for the random linear dynamical system in (62). (a), (b) Outlier-free data. (c), (d) Sampled data contaminated with outliers of magnitude 0.2 from  $t = 1$  to  $t = 1.05$  seconds.

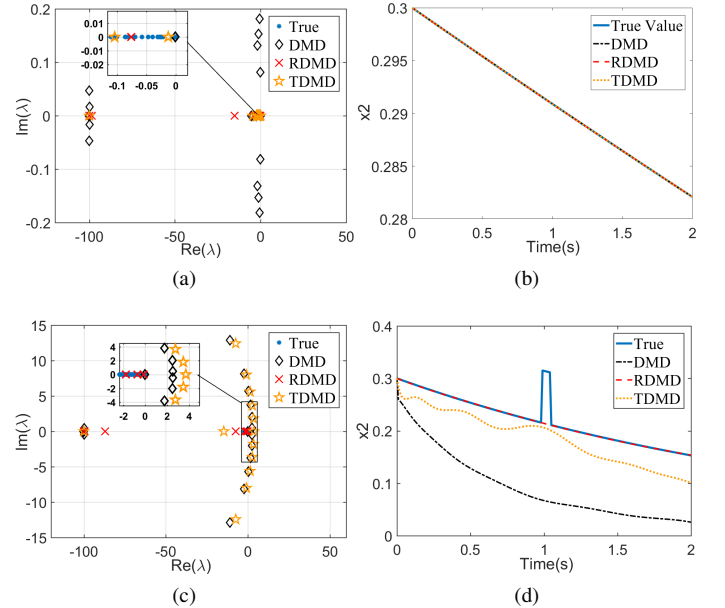


Fig. 9. Estimated eigenvalues and reconstruction of state  $x_2$  for the generalized slow-manifold system in (63). (a), (b) Outlier-free data. (c), (d) Sampled data contaminated with outliers of magnitude 0.2 from  $t = 1$  to  $t = 1.05$  seconds.

TABLE III  
COMPUTATION TIME (S) OF THE TESTED DMD METHODS

| Method    | B     | C     | D     | E     | F1    | F2    |
|-----------|-------|-------|-------|-------|-------|-------|
| DMD [33]  | 0.008 | 0.022 | 0.007 | 0.008 | 0.024 | 0.027 |
| TDMD [22] | 0.010 | 0.018 | 0.009 | 0.010 | 0.041 | 0.040 |
| ODMD [24] | 1.092 | 2.130 | 1.108 | 1.117 | —     | —     |
| N-RDMD    | 4.173 | 2.926 | 3.198 | 4.012 | 1.058 | 1.072 |

we assess the performance of the proposed N-RDMD in the presence of (a) Gaussian, (b) Laplace, (c) Student- $t$ , and (d)

Cauchy noise. The results are shown in Fig. 10. It is observed that the TDMD perform best for all noise types, followed by the proposed N-RDMD.

The superior performance of the TDMD is attributed to the symmetric de-biasing used by such a method, which makes it the best choice for noisy data. TDMD considers the uncertainties in both  $\mathbf{Y}$ ,  $\mathbf{Y}'$ , so that the problem becomes  $\mathbf{Y}' + \Delta\mathbf{Y}' = \mathbf{A}(\mathbf{Y} + \Delta\mathbf{Y})$ , whereas other methods consider only the uncertainties on the right-hand side of the problem. This explains why the TDMD performs best for noisy data and also, to a certain extent, suppress the effect of outliers in the estimation process. The combination that the TDMD and the proposed N-RDMD might offer is promising and left as a direction for future research.

### I. Comparison with Robust Least-Trimmed Square Dynamic Mode Decomposition

As discussed, a numerical method that is statistically robust was proposed in [25]. This method works based on a LTS estimator; thus, we refer to it as LTS-RDMD. The discussion on the efficiency and applicability of LTS estimators is given in the introduction. As stated, generalized maximum-likelihood estimators are easier to implement and faster to calculate with respect to LTS estimators. Consider a two-dimensional dynamical system as

$$\dot{\mathbf{x}}(t) = \begin{bmatrix} 1 & -2 \\ 1 & -1 \end{bmatrix} \mathbf{x}(t) \quad (64)$$

The measurement snapshots are contaminated with the additive deviation  $\eta\mathbf{w}(t) + \mu\mathbf{s}(t)$ , where  $\mathbf{w}(t)$  is the Gaussian noise. Also, the elements of the vector  $\mathbf{s}(t)$  are obtained by multiplying a Bernoulli trial with small expectation  $p$  by a standard normal, which leads to a sparse noise. Therefore, the snapshots are contaminated with a base Gaussian noise and some spikes of size  $\mu$  with firing rate  $p$  ([25]). The comparison between our RDMD and the LTS-RDMD to discover the eigenvalues of the system is given in Fig. 11. Note that we repeated the simulation 200 times for each method. Simulations are performed for fixed  $\mu = 1$  and  $p = 0.05$  and for two different Gaussian noises levels:  $\sigma = 10^{-4}$  and  $\sigma = 10^{-3}$ . The observation is that both methods can efficiently discover the true eigenvalues when the data are contaminated by the spikes (outliers). It can also be observed that, in a number of simulations, the LTS-RDMD finds some erroneous RHP eigenvalues, whereas RDMD always finds them near the true value. Moreover, Fig. 11 shows that the LTS-RDMD acts more precisely for higher levels of the Gaussian noise. The price for such additive robustness is the higher implementational and computational complexity of the LTS-RDMD. As stated in the previous subsection, the combination of the TDMD and the proposed RDMD could further improve the robustness in cases of more powerful Gaussian noise and will be addressed in our future research.

## V. CONCLUSIONS

The problem of making DMD robust to outliers is investigated and solved. By casting the DMD problem in the

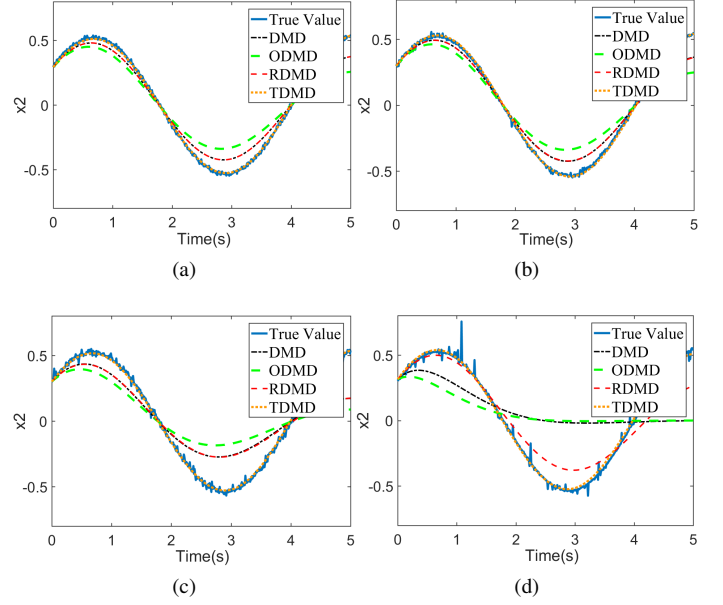


Fig. 10. State reconstruction of linear system (59) when the sampled data are contaminated with (a) Gaussian noise with variance of 0.01. (b) Laplacian noise with variance of 0.01. (c) Student-t noise with 2 degrees of freedom. (d) Cauchy noise with half-width at half-maximum  $\gamma = 2$ .

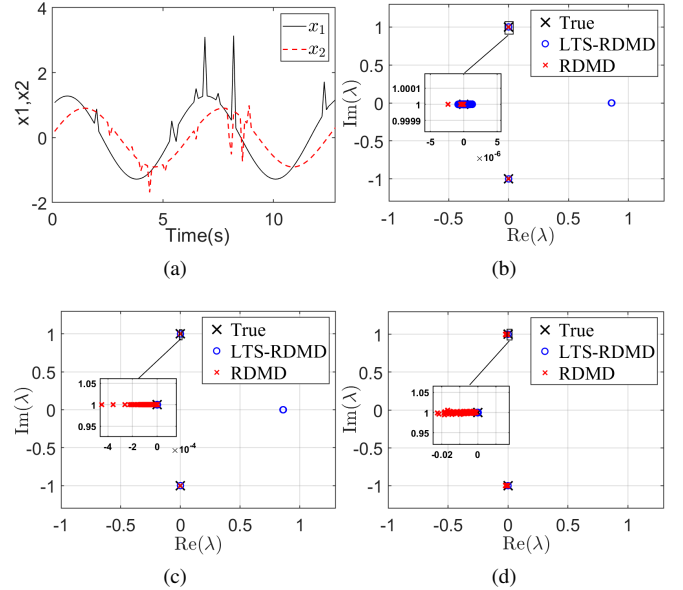


Fig. 11. Calculation of eigenvalues by RDMD and LTS-RDMD for the simple oscillator (64) in the following cases: (a) the measured data with noise and spikes; (b) discovered eigenvalues for noise-free data with spike levels  $\mu = 1$ ,  $p = 0.05$ ; (c) discovered eigenvalues with spike levels  $\mu = 1$ ,  $p = 0.05$  and Gaussian noise level  $\eta = 10^{-4}$ ; (d) discovered eigenvalues with spike levels  $\mu = 1$ ,  $p = 0.05$  and Gaussian noise level  $\eta = 10^{-3}$ .

robust statistics framework, we were able to solve it by using a SHGM estimator. The numerical results demonstrated the effectiveness of the proposed RDMD for a variety of dynamical systems when the sampled data are contaminated with outliers. Further, the proposed RDMD presented a satisfactory performance in dealing with non-Gaussian noises. Finally, we noticed that the numerical results are significantly improved by

considering the symmetry of the problem; thus, we suggest the robustification of the total least-squares method as a direction for future research.

## REFERENCES

- [1] T. Hey, S. Tansley, and K. Tolle, *The Fourth Paradigm: Data-Intensive Scientific Discovery*. Microsoft Research, 2009.
- [2] S. L. Brunton and J. N. Kutz, *Data-Driven Science and Engineering: Machine Learning, Dynamical Systems, and Control*. Cambridge University Press, 2019.
- [3] P. Schmid and J. Sesterhenn, “Dynamic mode decomposition of numerical and experimental data,” in *Sixty-First Annual Meeting of the APS Division of Fluid Dynamics*, San Antonio, Texas, USA, 2008.
- [4] C. W. Rowley, I. Mezić, S. Bagheri, P. Schlatter, and D. S. Henningson, “Spectral analysis of nonlinear flows,” *Journal of Fluid Mechanics*, vol. 641, p. 115–127, 2009.
- [5] J. N. Kutz, S. L. Brunton, B. W. Brunton, and J. L. Proctor, *Dynamic Mode Decomposition: Data-Driven Modeling of Complex Systems*. SIAM, 2016.
- [6] A. Mauroy, I. Mezić, and Y. Susuki (Editors), *The Koopman Operator in Systems and Control: Concepts, Methodologies, and Applications*. Cham, Switzerland: Springer Nature Switzerland AG, 2020.
- [7] Y. Susuki and I. Mezić, “Nonlinear Koopman modes and coherency identification of coupled swing dynamics,” *IEEE Transactions on Power Systems*, vol. 26, no. 4, pp. 1894–1904, 2011.
- [8] B. W. Brunton, L. A. Johnson, J. G. Ojemann, and J. N. Kutz, “Extracting spatial-temporal coherent patterns in large-scale neural recordings using dynamic mode decomposition,” *Journal of Neuroscience Methods*, vol. 258, pp. 1–15, 2016.
- [9] J. Mann and J. N. Kutz, “Dynamic mode decomposition for financial trading strategies,” *Quantitative Finance*, vol. 16, no. 11, pp. 1643–1655, 2016.
- [10] J. N. Kutz, X. Fu, and S. L. Brunton, “Multiresolution dynamic mode decomposition,” *SIAM Journal on Applied Dynamical Systems*, vol. 15, no. 2, pp. 713–735, 2016.
- [11] A. M. Avila and I. Mezić, “Data-driven analysis and forecasting of highway traffic dynamics,” *Nature Communications*, vol. 11, no. 1, p. 2090, 2020.
- [12] J. L. Proctor, S. L. Brunton, and J. N. Kutz, “Dynamic mode decomposition with control,” *SIAM Journal on Applied Dynamical Systems*, vol. 15, no. 1, pp. 142–161, 2016.
- [13] S. L. Brunton, B. W. Brunton, J. L. Proctor, E. Kaiser, and J. N. Kutz, “Chaos as an intermittently forced linear system,” *Nature Communications*, vol. 8, no. 1, p. 19, 2017.
- [14] S. Klus, P. Gelß, S. Peitz, and C. Schütte, “Tensor-based dynamic mode decomposition,” *Nonlinearity*, vol. 31, no. 7, pp. 3359–3380, jun 2018.
- [15] P. J. Huber, “Robust estimation of a location parameter,” *The Annals of Mathematical Statistics*, vol. 35, no. 1, pp. 73–101, 1964.
- [16] P. J. Rousseeuw and A. M. Leroy, *Robust Regression and Outlier Detection*, 1st ed., ser. Wiley Series in Probability and Statistics. Wiley, Feb. 2005.
- [17] R. A. Maronna, R. D. Martin, V. J. Yohai, and M. Salibián-Barrera, *Robust Statistics: Theory and Methods (with R)*, 2nd ed., ser. Wiley Series in Probability and Statistics. Wiley, Jan. 2019.
- [18] D. Duke, J. Soria, and D. Honnery, “An error analysis of the dynamic mode decomposition,” *Experiments in Fluids*, vol. 52, no. 2, pp. 529–542, 2012.
- [19] H. Zhang, S. T. M. Dawson, C. W. Rowley, E. A. Deem, and L. N. Cattafesta, “Evaluating the accuracy of the dynamic mode decomposition,” *Journal of Computational Dynamics*, vol. 7, no. 1, p. 35, 2020.
- [20] H. Lu and D. M. Tartakovsky, “Prediction accuracy of dynamic mode decomposition,” *SIAM Journal on Scientific Computing*, vol. 42, no. 3, pp. A1639–A1662, 2020.
- [21] S. T. M. Dawson, M. S. Hemati, M. O. Williams, and C. W. Rowley, “Characterizing and correcting for the effect of sensor noise in the dynamic mode decomposition,” *Experiments in Fluids*, vol. 57, no. 3, p. 42, 2016.
- [22] M. S. Hemati, C. W. Rowley, E. A. Deem, and L. N. Cattafesta, “De-biasing the dynamic mode decomposition for applied Koopman spectral analysis of noisy datasets,” *Theoretical and Computational Fluid Dynamics*, vol. 31, no. 4, pp. 349–368, 2017.
- [23] K. K. Chen, J. H. Tu, and C. W. Rowley, “Variants of dynamic mode decomposition: Boundary condition, Koopman, and Fourier analyses,” *Journal of Nonlinear Science*, vol. 22, no. 6, pp. 887–915, 2012.
- [24] S. Sinha, B. Huang, and U. Vaidya, “On robust computation of Koopman operator and prediction in random dynamical systems,” *Journal of Nonlinear Science*, vol. 30, no. 5, pp. 2057–2090, 2020.
- [25] T. Askham, P. Zheng, A. Aravkin, and J. N. Kutz, “Robust and scalable methods for the dynamic mode decomposition,” *preprint, arXiv:1712.01883v1*, 2017.
- [26] P. J. Rousseeuw, “Multivariate estimation with high breakdown point,” *Mathematical statistics and applications*, vol. 8, no. 283–297, p. 37, 1985.
- [27] L. Mili, M. G. Cheniae, N. S. Vichare, and P. J. Rousseeuw, “Robust state estimation based on projection statistics [of power systems],” *IEEE Transactions on Power Systems*, vol. 11, no. 2, pp. 1118–1127, 1996.
- [28] M. A. Gandhi and L. Mili, “Robust Kalman filter based on a generalized maximum-likelihood-type estimator,” *IEEE Transactions on Signal Processing*, vol. 58, no. 5, pp. 2509–2520, 2010.
- [29] M. Netto, J. Zhao, and L. Mili, “A robust extended Kalman filter for power system dynamic state estimation using pmu measurements,” in *2016 IEEE Power and Energy Society General Meeting (PESGM)*, 2016, pp. 1–5.
- [30] J. Zhao, M. Netto, and L. Mili, “A robust iterated extended Kalman filter for power system dynamic state estimation,” *IEEE Transactions on Power Systems*, vol. 32, no. 4, pp. 3205–3216, 2017.
- [31] M. Netto and L. Mili, “Robust Koopman operator-based Kalman filter for power systems dynamic state estimation,” in *2018 IEEE Power and Energy Society General Meeting (PESGM)*, 2018, pp. 1–5.
- [32] M. Netto and L. Mili, “A robust data-driven Koopman Kalman filter for power systems dynamic state estimation,” *IEEE Transactions on Power Systems*, vol. 33, no. 6, pp. 7228–7237, 2018.
- [33] P. J. Schmid, “Dynamic mode decomposition of numerical and experimental data,” *Journal of Fluid Mechanics*, vol. 656, p. 5–28, 2010.
- [34] J. H. Tu, C. W. Rowley, D. M. Luchtenburg, S. L. Brunton, and J. N. Kutz, “On dynamic mode decomposition: Theory and applications,” *Journal of Computational Dynamics*, vol. 1, no. 2, pp. 391–421, 2014.
- [35] A. Mauroy and I. Mezić, “Global stability analysis using the eigenfunctions of the Koopman operator,” *IEEE Transactions on Automatic Control*, vol. 61, no. 11, pp. 3356–3369, 2016.
- [36] B. O. Koopman, “Hamiltonian systems and transformation in Hilbert space,” *Proceedings of the National Academy of Sciences*, vol. 17, no. 5, pp. 315–318, 1931.
- [37] P. J. Rousseeuw and B. C. van Zomeren, “Unmasking multivariate outliers and leverage points,” *Journal of the American Statistical Association*, vol. 85, no. 411, pp. 633–639, 1990.
- [38] P. J. Rousseeuw and C. Croux, “Alternatives to the median absolute deviation,” *Journal of the American Statistical Association*, vol. 88, no. 424, pp. 1273–1283, 1993.
- [39] D. L. Donoho, “Breakdown properties of multivariate location estimators,” *Qualifying paper, Dept. Statistics, Harvard University*, 1982.
- [40] D. L. Donoho and M. Gasko, “Breakdown properties of location estimates based on halfspace depth and projected outlyingness,” *The Annals of Statistics*, vol. 20, no. 4, pp. 1803–1827, 1992.
- [41] C. Croux and P. J. Rousseeuw, “Time-efficient algorithms for two highly robust estimators of scale,” in *Computational Statistics*, Y. Dodge and J. Whittaker, Eds. Springer-Verlag, 1992, vol. 1, pp. 411–428.
- [42] M. Gasko and D. L. Donoho, “Influential observation in data analysis,” *American Statistical Association Proceedings of the Business and Economic Statistics Section*, pp. 104–109, 1982.
- [43] R. A. Willoughby, “Solutions of Ill-Posed Problems (A. N. Tikhonov and V. Y. Arsenin),” *SIAM Review*, vol. 21, no. 2, pp. 266–267, 1979.
- [44] L. Mili and C. W. Coakley, “Robust estimation in structured linear regression,” *The Annals of Statistics*, vol. 24, no. 6, pp. 2593–2607, 1996.
- [45] M. Netto and L. Mili, “Robust data filtering for estimating electromechanical modes of oscillation via the multichannel Prony method,” *IEEE Transactions on Power Systems*, vol. 33, no. 4, pp. 4134–4143, 2018.